



Published in final edited form as:

Conf Comput Commun Secur. 2017 ; 2017: 2421–2434. doi:10.1145/3133956.3134038.

Leaky Cauldron on the Dark Land: Understanding Memory Side-Channel Hazards in SGX

Wenhao Wang^{*}, Guoxing Chen[†], Xiaorui Pan^{*}, Yinqian Zhang[†], XiaoFeng Wang^{*}, Vincent Bindschaedler[†], Haixu Tang^{*}, and Carl A. Gunter[‡]

^{*} Indiana University, Bloomington, ww31@indiana.edu, xiaopan@indiana.edu, xw7@indiana.edu, hatang@indiana.edu

[†] The Ohio State University, chenguo@cse.ohio-state.edu, yinqian@cse.ohio-state.edu

[‡] University of Illinois at Urbana-Champaign, bindsch2@illinois.edu, cgunter@illinois.edu

Abstract

Side-channel risks of Intel’s SGX have recently attracted great attention. Under the spotlight is the newly discovered page-fault attack, in which an OS-level adversary induces page faults to observe the page-level access patterns of a protected process running in an SGX enclave. With almost all proposed defense focusing on this attack, little is known about whether such efforts indeed raises the bar for the adversary, whether a simple variation of the attack renders all protection ineffective, not to mention an in-depth understanding of other attack surfaces in the SGX system. In the paper, we report the first step toward systematic analyses of side-channel threats that SGX faces, focusing on the risks associated with its memory management. Our research identifies 8 potential attack vectors, ranging from TLB to DRAM modules. More importantly, we highlight the common misunderstandings about SGX memory side channels, demonstrating that high frequent AEXs can be avoided when recovering EdDSA secret key through a new page channel and fine-grained monitoring of enclave programs (at the level of 64B) can be done through combining both cache and cross-enclave DRAM channels. Our findings reveal the gap between the ongoing security research on SGX and its side-channel weaknesses, redefine the side-channel threat model for secure enclaves, and can provoke a discussion on when to use such a system and how to use it securely.

I. Introduction

A grand security challenge today is how to establish a trusted execution environment (TEE) capable of protecting large-scale, data-intensive computing. This is critical for the purposes such as outsourcing analysis of sensitive data (e.g., electronic health records) to an untrusted cloud. Serving such purposes cannot solely rely on cryptographic means, for example, fully homomorphic encryption, which is still far too slow to handle the computing task of a practical scale. A promising alternative is made possible by recent hardware progress such as Intel’s Software Guard Extension (SGX) [10]. SGX offers protection for data and code with a secure *enclave* designed to be resilient to attacks from its host operating system or

even system administrators. Such protection is offered as a feature of Intel’s mainstream CPUs (i.e., Skylake and Kaby Lake), and characterized by its small trusted computing base (TCB), including just the CPU package, and the potential to scale its performance with the capability of the processors. However, the simplicity of the design forces an enclave program to utilize resources (memory, I/O, etc.) partially or fully controlled by the untrusted OS, and therefore potentially subjects it to *side-channel* attacks, in which the adversary outside the enclave could *infer* sensitive information inside from observed operations on the shared resources.

SGX side-channel hazards.

Unfortunately, the threat has been found to be more realistic and serious than thought: prior studies have shown that an adversary with a full control of the OS can manipulate the page tables of the code running in the enclave-mode—a CPU mode protected by SGX—to induce page faults during its execution; through monitoring the occurrences of the faults in a relatively noise-free environment created by the adversary, he could identify the program’s execution trace at the page level, which is shown to be sufficient for extracting text documents, outlines of images from popular application libraries [39] and compromising cryptographic operations [35]. In our paper, we call these attacks the page-fault side-channel attacks.

Intel’s position on these side-channel attacks offers much food for thought. They admit that SGX does not defend against four side-channel attack vectors: power statistics, cache miss statistics, branch timing and page accesses via page tables [2]. Facing the security threats due to these side channels, Intel recommends that “it would be up to the independent software vendors to design the enclave in a way that prevents the leaking of side-channel information. [7]”, though they actually work actively with academia and open source partners to help mitigate the threats [6].

It is clear, from Intel’s statements, radical hardware changes to address these side-channel problems (e.g., defeating page-fault side channels by keeping the entire page tables inside the enclave [15]) is unlikely to happen. As a result, software vendors are left with the daunting tasks of understanding the security impacts of the SGX side channels and developing practical techniques to mitigate the threats when building their SGX applications.

Given the importance of the problem, recent years have already witnessed mushrooming of the attempts to address SGX side channel threats [35], [34], [14], for example, by placing sensitive code and data within the same page [35], or by detecting page faults through hardware supports [34] or timed-execution [14]. However, these studies were primarily targeting the page-fault attacks. Although the concern about this demonstrated attack vector is certainly justified, the sole attention on the page-fault attack can be inadequate. After all, tasking a safe heaven built upon minimum software support with complicated computing missions (e.g., data-intensive computing) can potentially open many avenues for inside information to trickle out during the interactions with the outside, when the external help is needed to accomplish the missions. Focusing on memory alone, we can see not only a program’s virtual memory management but that its physical memory control are partially or

fully exposed to the untrusted OS, not to mention other system services an enclave program may require (process management, I/O, etc.). Even only looking at page tables, we are not sure whether the known paging attack is the only or the most effective way to extract sensitive information from the enclave process. In the absence of a comprehensive understanding of possible attack surfaces, it is not clear at all whether all proposed protection, which tends to be heavyweight and intrusive, can even raise the bar to side-channel attacks, and whether an adversary can switch to a different technique or channel, more lightweight and equally effective, to extract the information these approaches were designed to protect.

Understanding memory side channels.

As a first step towards a complete understanding of all side-channel threats software vendors face, in this paper, we focus on memory-related side channels, which is an important, and arguably the most effective, category of side channels that have ever been studied. Of course, the page-fault side channel falls in the scope of our discussion. To deepen the community's understanding of the memory side-channel attack surfaces and guide the design of defense mechanisms, we particularly hope to convey the following *three* messages through this paper. First, *page faults are not the only vector that leaks enclave program's memory access patterns*. Any follow-up attempt to mitigate memory side-channel leaks should take into account the entire attack surfaces. Second, *not every side-channel attack on enclave induces a large number of Asynchronous Enclave eXits (AEXs) as demonstrated in the page-fault attacks*. This is important because the anomalously high AEX interrupt rate has been considered to be a key feature of SGX side-channel attacks, which can be defeated by the protection designed to capture this signal [34], [14]. Our finding, however, shows that such interrupt-based protection is fragile, as more sophisticated attacks can avoid producing too many interrupts. Third, *it is possible to get a finer-grained (i.e., at the cache-line granularity) side-channel observation into the enclave memory*. Hence, defense that place sensitive code and data on the same page [35] will not be effective on the new attacks.

In this paper, we hope to get across these messages through the following research efforts:

- *Systematically exploring memory side-channel attack surfaces*. Our study aims to provide a systematic exploration of SGX side-channel attack vectors involving memory management. Particularly, we enumerate total 8 types of side-channel attack vectors that relate to address translation caches in CPU hardware (e.g., TLB, paging-structure caches), page tables located in the main memory, and the entire cache and DRAM hierarchy. This categorization considers each step in the address translation and memory operation, thus to our knowledge presents the most comprehensive analysis on memory side-channel attack surfaces against SGX enclaves.
- *Reducing side effects of memory side-channel attacks*. To demonstrate that a large number of AEXs is *not* a necessary condition of memory side-channel attacks, we develop a new memory-based attack, called *sneaky page monitoring* (SPM). SPM attacks work by setting and resetting a page's *accessed* flag in the page table entry (PTE) to monitor when the page is visited. Unlike the page-fault attacks [39], in which a page fault is generated each time when a page is accessed, manipulation of the *accessed* flags does not trigger any interrupt

directly. However, the attack still needs to flush the *translation lookaside buffer* (TLB) from time to time by triggering interrupts to force the CPU to look up page tables and set *accessed* flags in the PTEs. Nevertheless, we found that there are several ways to reduce the number of the interrupts or even completely eliminate them in such attacks. Particularly, we can avoid tracking the access patterns between the entry and exit pages of a program fragment (e.g., a function) and instead, use the *execution time* measured between these pages to infer the execution paths in-between. This approach can still work if all secret-dependent branches are located in the same page (i.e., a mechanism proposed by [35]), as long as there is still a timing difference between the executions of these branches. Further, we present a technique that utilizes Intel's HyperThreading capability to flush the TLBs through an attack process sharing the same CPU core with the enclave code, which can eliminate the need of interrupts, when HyperThreading is on.

We demonstrate the effectiveness of SPM through attacks on real-world applications. Particularly, we show that when attacking EdDSA (Section IV-C), our timing enhancement only triggers 1,300 interrupts, compared with 71,000 caused by the page-fault attack and 33,000 by the direct *accessed* flags attack, when recovering the whole 512-bit secret key. This level of the interrupt rate makes our attack almost invisible to all known interrupt-based defense [34], [14], given the fact that even normal execution of the target program generates thousands of interrupts.

- *Improving attack's spatial granularity.* Page-fault attacks allow attackers to observe the enclave program's memory access pattern at the page granularity (4KB), therefore existing solutions propose to defeat the attacks by aligning sensitive code and data within the same memory pages. To show that this defense strategy is ineffective, we demonstrate a series of memory side-channel attacks that achieve finer spatial granularity, which includes a cross-enclave PRIME+PROBE attack, a cross-enclave DRAMA attack, and a novel cache-DRAM attack. Particularly, the cache-DRAM attack leverages both PRIME+PROBE cache attacks and DRAMA attacks to improve the spatial granularity. When exploiting both channels, we are able to achieve a fine-grained observation (64B vs. 16KB for PRIME+PROBE and >1KB for the DRAM attack alone), which enables us to monitor the execution flows of an enclave program (similar to FLUSH+RELOAD attacks). Note that this cannot be done at the cache level since in our case the attacker does not share code with the target enclave program, which makes FLUSH+RELOAD impossible.

Implications.

Our findings point to the disturbing lack of understanding about potential attack surfaces on SGX, which can have a serious consequence. Not only are all existing defense mechanisms vulnerable to the new attacks we developed, but some of them only marginally increase the cost on the attacker side: as demonstrated in our study, for the channels on the virtual memory, the page-fault attack is not the most cost-effective one and a large number of AEX interrupts are *not* necessary for a successful attack; all existing protection does not add much burden to a more sophisticated attacker, who can effectively reduce the frequency of AEXs without undermining the effectiveness of the attack. Most importantly, we hope that our

study can lead to rethinking the security limitations of SGX and similar TEE technologies, provoking a discussion on when to use them and how to use them properly.

Contributions.

In this paper, we make the following contributions:

- *First systematic study on SGX side-channel attack surfaces.* We report the first systematic exploration of the side-channel attack surfaces on Intel SGX. Although only focusing on the memory management, our study reveals new channels that disclose information from the enclave, particularly *accessed flags*, timing and cross-enclave channels.
- *New attacks.* We developed a suite of new attack techniques that exploit these new channels. Particularly, we show multiple channels can complement each other to enhance the effectiveness of an attack: timing+*accessed flags* to reduce AEXs (rendering existing protection less effective) and DRAM+Cache to achieve a fine-grained observation into the enclave (64B).
- *New understanding.* We discuss possible mitigations of the new threats and highlight the importance in better understanding the limitations of SGX-like technologies.

II. Background

A. Memory Isolation in Intel SGX

Memory isolation of enclave programs is a key design feature of Intel SGX. To maintain backward-compatibility, Intel implements such isolation via extensions to existing processor architectures, which we introduce below.

Virtual and physical memory management.—Intel SGX reserves a range of continuous physical memory exclusively for enclave programs and their control structures, dubbed Processor Reserved Memory (PRM). The extended memory management units (MMU) of the CPU prevents accesses to the PRM from all programs outside enclaves, including the OS kernel, virtual machine hypervisors, SMM code or Direct Memory Accesses (DMA). Enclave Page Cache (EPC) is a subset of the PRM memory range. The EPC is divided to pages of 4KBs and managed similarly as the rest of the physical memory pages. Each EPC page can be allocated to one enclave at one time.

The virtual memory space of each program has an Enclave Linear Address Range (ELRANGE), which is reserved for enclaves and mapped to the EPC pages. Sensitive code and data is stored within the ELRANGE. Page tables responsible for translating virtual addresses to physical addresses are managed by the untrusted system software. The translation lookaside buffer (TLB) works for EPC pages in traditional ways. When the CPU transitions between *non-enclave mode* and *enclave mode*, through `EENTER` or `EEXIT` instructions or Asynchronous Enclave Exits (AEXs), TLB entries associated with the current Process-Context Identifier (PCID) as well as the global identifier are flushed, preventing non-enclave code learning information about address translation inside the enclaves.

Security check for memory isolation.—To prevent system software from arbitrarily controlling the address translation by manipulating the page table entries, the CPU also consults the Enclave Page Cache Map (EPCM) during the address translation. Each EPC page corresponds to an entry in the EPCM, which records the owner enclave of the EPC page, the type of the page, and a valid bit indicating whether the page has been allocated. When an EPC page is allocated, its access permissions are specified in its EPCM entry as *readable*, *writable*, and/or *executable*. The virtual address (within ELRANGE) mapped to the EPC page is also recorded in the EPCM entry.

Correctness of page table entries set up by the untrusted system software is guaranteed by an extended Page Miss Handler (PMH). When the code is executing in the enclave mode or the address translation result falls into the PRM range, additional security check will take place. Specially, when the code is running in the non-enclave mode and address translation falls into the PRM range, or the code runs in the enclave mode but the physical address is not pointing to a *regular* EPC page belonging to the current enclave, or the virtual address triggering the page table walk doesn't match the virtual address recorded in the corresponding entry in the EPCM, a page fault will occur. otherwise, the generated TLB entries will be set according to both the attributes in the EPCM entry and the page table entry.

Memory encryption.—To support larger ELRANGE than EPC, EPC pages can be “swapped” out to regular physical memory. This procedure is called EPC page eviction. The confidentiality and integrity of the evicted pages are guaranteed through authenticated encryption. The hardware Memory Encryption Engine (MEE) is integrated with the memory controller and seamlessly encrypts the content of the EPC page that is evicted to a regular physical memory page. A Message Authentication Code (MAC) protects the integrity of the encryption and a nonce associated with the evicted page. The encrypted page can be stored in the main memory or swapped out to secondary storage similar to regular pages. But the metadata associated with the encryption needs to be kept by the system software properly for the page to be “swapped” into the EPC again.

B. Adversary Model

In this paper, we consider attacks against enclave-protected code and data. The system software here refers to the program that operates with system privileges, such as operating systems and hypervisors. Our focus in this paper is side-channel analysis that threatens the confidentiality of the enclave programs. As such, software bugs in the code of an enclave program are out of our scope. Moreover, side channels not involving memory management and address translation are not covered either.

We assume in our demonstrated attacks knowledge of the victim binary code to be loaded into the enclave. As the adversary also knows the base address of the enclave binary in the virtual address space, as well as the entire virtual-to-physical mapping, the mapping of the binary code in pages, caches, DRAMs can be derived. Source code of the victim program is NOT required. We conducted analysis and experiments on *real* SGX platforms. So we do

assume the adversary has access to a machine of the same configuration before performing the attacks.

III. Understanding Attack Surfaces

In this section, we explore side-channel attack surfaces on Intel SGX, through systematic enumeration of attack vectors (shared resources that allow interference of the execution inside enclaves), followed by an analysis of individual vectors, in terms of the way they can be exploited and effectiveness of the attacks.

A. Attack Vectors

A memory reference in the modern Intel CPU architectures involves a sequence of micro-operations: the virtual address generated by the program is translated into the physical address, by first consulting a set of address translation caches (e.g., TLBs and various paging-structure caches) and then walking through the page tables in the memory. The resulting physical address is then used to access the cache (e.g., L1, L2, L3) and DRAM to complete the memory reference. Here, we discuss memory side-channel attack vectors in each of these steps.

Address Translation Caches.—Address translation caches are hardware caches that facilitate address translation, including TLBs and various paging-structure caches. TLB is a multi-level set-associative hardware cache that temporarily stores the translation from virtual page numbers to physical page numbers. Specially, the virtual address is first divided into three components: TLB tag bits, TLB-index bits, and page-offset bits. The TLB-index bits are used to index a set-associative TLB and the TLB-tag bits are used to match the tags in each of the TLB entries of the searched TLB set. Similar to L1 caches, the L1 TLB for data and instructions are split into dTLB and iTLB. An L2 TLB, typically larger and unified, will be searched upon L1 TLB misses. Recent Intel processors allow selectively flushing TLB entries at context switch. This is enabled by the Process-Context Identifier (PCID) field in the TLB entries to avoid flushing the entries that will be used again. If both levels of TLBs miss, a page table walk will be initiated. The virtual page number is divided into, according to Intel's terminology, PML4 bits, PDPTE bits, PDE bits, and PTE bits, each of which is responsible for indexing one level of page tables in the main memory. Due to the long latency of page-table walks, if the processor is also equipped with paging structure caches, such as PML4 cache, PDPTE cache, PDE cache, these hardware caches will also be searched to accelerate the page-table walk. The PTEs can be first searched in the cache hierarchy before the memory access [11].

Vector 1: Shared TLBs and paging-structure caches under HyperThreading.

When HyperThreading (HT)¹ is enabled, code running in the enclave mode may share the same set of TLBs and paging-structure caches with code running in non-enclave mode. Therefore, the enclave code's use of such resources will interfere with that of the non-

¹Intel's term for Simultaneous Multi-Threading.

enclave code, creating side channels. This attack vector is utilized to clear the TLB entries in the HT-SPM attack (Section IV-A).

Vector 2: Flushing selected entries in TLB and paging-structure caches at AEX.

According to recent versions of Intel Software Developer's Manual [3], entering and leaving the enclave mode will flush entries in TLB and paging-structure caches that are associated with the current PCID. As such, it enables an adversary from a different process context to infer the flushed entries at context switch. This is possible even on processors without HT. However, we were not able to confirm this attack vector on the machines we had (i.e., Skylake i7-6700). We conjecture that this is because our Skylake i7-6700 follows the specification in an older version of Intel Software Developer's Manual [4], which states all entries will be flushed regardless of the process context. Nevertheless, we believe this attack vector could be present in future processors.

Vector 3: Referenced PTEs are cached as data.

Beside paging-structure caches, referenced PTEs will also be cached as regular data [11]. This artifact enables a new attack vector: by exploiting the FLUSH+RELOAD side channel on the monitored PTEs, the adversary can perform a cross-core attack to trace the page-level memory access pattern of the enclave code. This attack vector presents a timing-channel version of the sneaky page monitoring attack we describe in Section IV. We will discuss its implication in Section VI.

Page tables.—Page tables are multi-level data structures stored in main memory, serving address translation. Every page-table walk involves multiple memory accesses. Different from regular memory accesses, page-table lookups are triggered by the micro-code of the processor direction, without involving the re-ordering buffer [11]. The entry of each level stores the pointer to (i.e., physical address of) the memory page that contains the next level of the page table. The structure of a PTE is shown in Figure 1. Specially, bit 0 is *present* flag, indicating whether a physical page has been mapped to the virtual page; bit 5 is *accessed* flag, which is set by the processor every time the page-table walk leads to the reference of this page table entry; bit 6 is *dirty* flag, which is set when the corresponding page has been updated. Page frame reclaiming algorithms rely on the *dirty* flag to make frame reclamation decisions.

As the page tables are located inside the OS kernel and controlled by the untrusted system software, they can be manipulated to attack enclaves. However, as mentioned earlier, because the EPC page permission is also protected by EPCM, malicious system software cannot arbitrarily manipulate the EPC pages to compromise its integrity and confidentiality. However, it has been shown in previous work [39] that by clearing the *present* flag in the corresponding PTEs, the malicious system software can collect traces of page accesses from the enclave programs, inferring secret-dependent control flows or data flows. Nevertheless, setting *present* flag is not the only attack vector against enclave programs.

Vector 4: Updates of the *accessed* flags in enclave mode.

When the page-table walk results in a reference of the PTE, the *accessed* flag of the entry will be set to 1. As such, code run in non-enclave mode will be able to detect the page table updates and learn that the corresponding EPC page has just been visited by the enclave code. However, page-table walk will also update TLB entries, so that future references to the same page will not update the *accessed* flags in PTEs, until the TLB entries are evicted by other address translation activities. We exploit this attack vector in our SPM attacks in Section IV.

Vector 5: Updates of the *dirty* flags in enclave mode.

Similar to *accessed* flags, the *dirty* flag will be updated when the corresponding EPC page is modified by the enclave program. This artifact can be exploited to detect memory writes to a new page. The new side-channel attack vector will enable the adversary to monitor secret-dependent memory writes, potentially a finer-grained inference attack than memory access tracking.

Vector 6: Page faults triggered in enclave mode.

In addition to the *present* flag, a few other bits in the PTEs can be exploited to trigger page faults. For example, on a x86-64 processor, bit M to bit 51 are reserved bits which when set will trigger page fault upon address translation. Here bit $M - 1$ is the highest bit of the physical address on the machine. The *NX* flag, when set, will force page faults when instructions are fetched from the corresponding EPC page.

Cache and memory hierarchy.—Once the virtual address is translated into the physical address, the memory reference will be served from the cache and memory hierarchy. Both are temporary storage that only hold data when the power is on. On the top of the hierarchy is the separate L1 data and instruction caches, the next level is the unified L2 cache dedicated to one CPU core, then L3 cache shared by all cores of the CPU package, then the main memory. Caches are typically built on Static Random-Access Memory (SRAM) and the main memory on Dynamic Random-Access Memory (DRAM). The upper level storage tends to be smaller, faster and more expensive, while the lower level storage is usually larger, slower and a lot cheaper. Memory fetch goes through each level from top to bottom; misses in the upper level will lead to accesses to the next level. Data or code fetched from lower levels usually update entries in the upper level in order to speed up future references.

The main memory is generally organized in multiple memory channels. Each memory channel is handled by a dedicated memory controller. One memory channel is physically partitioned into multiple DIMMs (Dual In-line Memory Module), each with one or two ranks. Each rank has several DRAM chips (e.g., 8 or 16), and is also partitioned into multiple banks. A bank carries the memory arrays organized in rows and each of the rows typically has a size of 8KB, shared by multiple 4KB memory pages since one page tends to span over multiple rows. Also on the bank is a *row buffer* that keeps the most recently accessed row. Every memory read will load the entire row into the row buffer before the memory request is served. As such, accesses to the DRAM row already in the row buffer are much faster.

Vector 7: CPU caches are shared between code in enclave and non-enclave mode.

SGX does not protect enclave against cache side-channel attacks. Therefore, all levels of caches are shared between code in enclave mode and non-enclave mode, similar to cross-process and cross-VM cache sharing that are well-known side-channel attack vectors. Therefore, all known cache side-channel attacks, including those on L1 data cache, L1 instruction cache, and L3 cache, all apply to the enclave settings. We empirically confirmed such threats (Section-V-A).

Vector 8: The entire memory hierarchy, including memory controllers, channels, DIMMs, DRAM ranks and banks (including row buffers), are shared between code in enclave and non-enclave mode.

Similar to cache sharing, DRAM modules are shared by all processes running in the computer systems. Therefore, it is unavoidable to have enclave code and non-enclave code accessing memory stored in the same DRAM bank. The DRAM row buffer can be served as a side-channel attack vector: when the target program makes a memory reference, the corresponding DRAM row will be loaded into the row buffer of the bank; the adversary can compare the row-access time to detect whether a specific row has just been visited, so as to infer the target's memory access. This artifact has been exploited in DRAMA attacks [32]. In Section V, we show that after key technical challenges are addressed, such attacks can also succeed on enclave programs. Other shared memory hierarchy can also create contention between enclave and non-enclave code, causing interference that may lead to covert channels [24].

B. Characterizing Memory Vectors

Here we characterize the aforementioned memory side-channels in three dimensions:

Spatial granularity.—This concept describes the smallest unit of information *directly* observable to the adversary during a memory side-channel attack. Specifically, it measures the size of the address space one side-channel observation could not reveal. For example, the spatial granularity of the page-fault attack is 4KB, indicating that every fault enables the adversary to see one memory page (4096 bytes) being touched, though the exact address visited is not directly disclosed.

Temporal observability.—Given a spatial granularity level, even though the adversary cannot directly see what happens inside the smallest information unit, still there can be *timing signals* generated during the execution of the target program to help distinguish different accesses made by the program within the unit. For example, the duration for a program to stay on a page indicates, indirectly, whether a single memory or multiple accesses occur. A side-channel is said to have this property if the timing is measured and used to refine the observations in the attack.

Side effects.—We use this concept to characterize observable anomalies caused by a memory side-channel attack, which could be employed to detect the attack. An example is AEX, which is frequently invoked by the page-fault attack. Another side effect is the

slowdown of the execution. Since the primary approach to conducting a side-channel attack is to cause contention in memory resource, such as the flush of caches, TLBs, paging structure caches, DRAM row buffers, etc., overheads will be introduced to the runtime performance of the enclave code. AEXs also contribute to the performance overhead. For example, the original page-fault attacks are reported to make the target program run one or two orders of magnitude slower. This level of slowdown is easy to get noticed. Frequent AEXs are also detectable using approaches proposed by Chen *et al.* [14], as the execution time between two basic blocks can be much longer.

IV. Reducing Side Effects with Sneaky Page Monitoring Attacks

To attack the virtual memory, a page-fault side-channel attacker first restricts access to all pages, which induces page faults whenever the enclave process touches any of these pages, thereby generating a sequence of its page visits. A problem here is that this approach is heavyweight, causing an interrupt for each page access. This often leads to a performance slowdown by one or two orders of magnitude [39]. As a result, such an attack could be detected by looking at its extremely high frequency of page faults (i.e., AEXs) and anomalously low performance observed from the remote. All existing solutions, except those requiring hardware changes, are either leveraging interrupts or trying to remove the page trace of a program (e.g., putting all the code on one page). Little has been done to question whether such defense is sufficient.

To show that excessive AEXs are not the necessary condition to conducting memory side-channel attack, in this section, we elaborate sneaky page monitoring (SPM), a new paging attack that can achieve comparable effectiveness with much less frequent AEXs.

A. The Three SPM Attacks (Vector 4)

In this section, we introduce three types of SPM attacks, which monitor the page table entries and exploit different techniques to flush TLBs.

B-SPM: Accessed Flags Monitoring.—The SPM attack manipulates and monitors the *accessed* flags on the pages of an enclave process to identify its execution trace. Specifically, we run a system-level attack process outside an enclave to repeatedly inspect each page table entry's *accessed* flag, record when it is set (from 0 to 1) and reset it once this happens. The page-access trace recovered in this way is a sequence of *page sets*, each of which is a group of pages visited (with their *accessed* flags set to 1) between two consecutive inspections. This attack is lightweight since it does not need any AEX to observe the pages first time when they are visited.

However, as mentioned earlier, after a virtual address is translated, its page number is automatically added to a TLB. As a result, the *accessed* flag of that page will not be set again when the page is visited later. To force the processor to access the PTE (and update the flag), the attacker has to invalidate the TLB entry proactively. The simplest way to do so is by generating an inter-processor interrupt (IPI) from a different CPU core to trigger a TLB shutdown, which causes an AEX from the enclave, resulting in flushing of all TLB entries of the current PCID. Figure 2 illustrates this attack, which we call *basic SPM* or *B-SPM*.

This B-SPM attack still involves interrupts but is already much more lightweight than page-fault attack: TLB shutdowns are typically less expensive than page faults; more importantly, B-SPM only triggers interrupts *when visiting the same page needs to be observed again*, while the latter needs to trigger an interrupt for *every (new) page access*.

In terms of accuracy, the page-fault attack tends to have a finer-grained observation while B-SPM attack cannot differentiate the visiting order of two pages that are spotted during the same round of inspections. However B-SPM attack strives for a balance between the interrupt rate and attack resolutions.

T-SPM: Timing enhancement.—When repeated visits to same pages become a salient feature for an input, the basic SPM needs to issue more TLB shutdowns in order to observe the feature, making the attack observable to the existing protections that detect the anomalous interrupt rate [34], [14], Figure 3 illustrates an example, in which the secret-dependent code resides in the same page, except that the execution on one condition involves a loop while that on the other does not, leading to different execution time. In this case, TLB shutdowns during the execution of the loop are required to distinguish two branches using page visit traces (i.e. number of page visits). To reduce the number of the interrupts, we leverage a timing channel to enhance SPM, making it stealthier. Specifically, given a code fragment with a unique entry page α and a unique exit page β , together with multiple input-dependent paths between the two points on different pages, our timing-enhanced SPM (called *T-SPM*) continuously monitors α and β , measuring the execution time between these two points, and once the *accessed* flag of β is found to be set, flushes the TLB and resets the *accessed* flags for both PTEs. The timing recorded is then used to infer the input of the code fragment.

This simple approach avoids all the interrupts between α and β , but still reveals the possible execution path connecting them. In the extreme case, when all other code stays on the same page, as proposed by the prior research [35] to defend against page-fault attacks, T-SPM can still infer sensitive information when the operations on them take different time to complete.

HT-SPM: TLB Flushing through HyperThreading.—Further we found that when HyperThreading is turned on for a processor, we can clear up the TLBs without issuing TLB shutdowns, which renders all existing interrupt-based protection ineffective.

HyperThreading runs two virtual cores on a physical core to handle the workloads from two different OS processes. This resource-sharing is transparent to the OS and therefore does not trigger any interrupt. The processes running on the two virtual cores share some of the TLBs, which allows the attacker to remove some TLB entries outside the enclave, without causing any interrupts. As a result, in the presence of HyperThreading, we can run an attack process together with an enclave process, to continuously probe the virtual addresses in conflict with the TLB entries the latter uses, in an attempt to evict these entries and force the victim process to walk its page tables. Using this technique, which we call *HT-SPM*, we can remove most or even eliminate the interrupts during an attack.

B. Evaluation of Effectiveness

Our analysis was performed on an Dell Optiplex 7040 with a Skylake i7-6700 processor and 4 physical cores, with 16GB memory. The configuration of the cache and memory hierarchy is shown in Table I. It runs Ubuntu 16.04 with kernel version 4.2.8. During our experiments, we patched the OS when necessary to facilitate the attacks, as an OS-level adversary would do. We used the latest Graphene-SGX Library OS [5], [37] compiled using GCC 5.4.0 with default compiling options to port unmodified libraries.

B-SPM on Hunspell.—Hunspell is a popular spell checking tool used by software packages like Apple’s OS X and Google Chrome. It stores a dictionary in a hash table, which uses linked lists to link the words with the same hash values. Each linked list spans across multiple pages, so searching for a word often generates a unique page-visit sequence. Prior study [39] shows that by monitoring page faults, the attacker outside an enclave can fingerprint the dictionary lookup function inside the enclave, and further determine the word being checked from the sequence of accessing different data pages (for storing the dictionary). In our research, we evaluated B-SPM on Hunspell 1.3.3 and found that the invocation of its `spell` function (looking up for one word) can be determined by the access of a specific page, which can be reliably identified at the inspection rate (for an attack process running on a separate core) of once per 184 CPU cycles. For simplicity, our attack process issues a TLB shutdown once the function invocation is discovered. In the interrupt, the process inspects the PTEs of pages being monitored to identify the searched word and resets their *accessed* flags, and then monitors for the occurrence of next function invocation. This approach identifies all the iterative lookups for multiple words.

Like the prior research [39], we also evaluated our attack using the `en_US` Hunspell dictionary, as illustrated in Table II. To compare with the page-fault attack, we reimplemented it and ran it against the same data-set, whose results are shown in Table II. As we can see here, the effectiveness of B-SPM is in line with that of the known attack: e.g., the percentage of the uniquely-identifiable words (i.e., group size 1) is 73.47% in our attack, a little below 83.05% observed in the page-fault attack; more than 92% of the words are in group size less than or equal to 3, compared with 98.6% in the page-fault attack. When it comes to performance, however, B-spM runs much faster: for 62,129 word look-ups it slowed down the original program by a factor of 5.1×, while the existing attack incurred an overhead of 1214.9×. Note that the prior research reports a slowdown of 25.1× for 39,719 word look-ups over the SGX emulator [39]. In our study, however, we ran both experiments on the *real* SGX platform.

T-SPM on FreeType.—FreeType is a font library that converts text content (the input) into images, which has been used by Linux, Android and iOS and other software packages. In our research, we ran T-SPM on its TrueType font rendering function, as did in the prior study [39]. The function, `TT_load_Glyph`, takes a letter’s glyph as its input to construct its bitmap. The prior study fingerprints the start and the end of the function, and selects a set of pages in-between and uses the number of page faults observed on these pages to determine the letter being rendered. In our research, we utilize a trigger page to identify the execution of the `TT_load_Glyph` function and then within the function, select 5 different α - β pairs

along its control-flow graph as features for identifying the 26 alphabet and the space between words (see Table III). Each feature, the timing between its α and β points, can separate some of these 27 letters from others. Collectively, they form a feature vector over which we run a Random Forest Classifier (with number of estimators set as 400) to classify an observed execution of *TT_load_Glyph* into one of these letters.

We ran our experiment on FreeType 2.5.3 within an enclave and collected 250 samples of a 1000 character paragraph from the book *The Princess and the Goblin* as a training set for the Random Forest Classifier. Then we tested on a 1000 character paragraph from *The Wonderful Wizard of Oz*, as is used in the prior study [39]. Based upon the timing vectors observed in the experiments (with an inspection rate of once per 482 cycles), our classifier correctly identified 57.35% of the letters with a precision of 89.94% (see Table IV), and 100% of the spaces. 72.14% of the words were correctly recovered by running a dictionary spelling check. Compared with the page-fault attack, which captured 100% of the words, T-SPM is less accurate but much more efficient: it incurred an overhead of 16%, while our re-implemented page-fault attack caused the program to slow down by a factor of 252 \times .

HT-SPM on Hunspell.—As an example, we ran HT-SPM on Hunspell, in a scenario when a set of words were queried on the dictionary. We conducted the experiments on the Intel Skylake i7-6700 processor, which is characterized by multi-level TLBs (see Table I). The experiments show that the dTLB and L2 TLB are fully *shared* across logical cores. Our attack process includes 6 threads: 2 *cleaners* operating on the same physical core as the Hunspell process in the enclave for evicting its TLB entries and 4 *collectors* for inspecting the *accessed* flags of memory pages. The cleaners probed all 64 and 1536 entries of the dTLB and L2 TLB every 4978 cycles and the collectors inspected the PTEs once every 128 cycles. In the experiment, we let Hunspell check 100 words inside the enclave, with the attack process running outside. The collectors, once seeing the fingerprint of the `spell` function, continuously gathered traces for data-page visits, from which we successfully recovered the exact page visit set for 88 words. The attack incurred a slowdown of 39.1% and did not fire a single TLB shutdown.

C. Silent Attacks on EdDSA

To understand the stealthiness of different attacks, in terms of their AEX frequency (which are used by the prior research to detect page side-channel attacks [34], [14]), we ran the page-fault attack, B-SPM and T-SPM against the latest version of Libcrypt (v1.7.6) to recover the EdDSA session keys². Edwards-curve Digital Signature Algorithm (EdDSA) [13] is a high-speed high-security digital signature scheme over twisted Edwards curves. The security of EdDSA is based on the difficulty of the well-known elliptic curve discrete logarithm problem: given points P and Q on a curve to find an integer a , if it exists, such that $Q = aP$. Provided the security parameters b and a cryptographic hash function H producing $2b$ -bit output, an EdDSA secret is a b -bit string k , and $a = H(k)$ is also private. The corresponding public key is $A = sB$, with B the base point and s the least significant b bits of

²The attacks only involve code pages, while HT-SPM is designed to reduce AEXs for data pages. As such, HT-SPM is not presented in the comparison.

a. Let r be the private session key, the signature of a message M under k is a $2b$ -bit string (R, S) , where $R = rB$ and $S = (r + H(R, A, M)a) \bmod l$. It can be seen that if r is disclosed, assuming $H(R, A, M) \bmod l \neq 0$, the long-term secret key a can be directly obtained as $a = (S - r)/H(R, A, M) \bmod l$.

Figure 4 presents the main function for ECC scalar point multiplication. Although Libgcrypt provides side-channel protection by tagging the long-term private key as “secure memory”, we found that it does not protect the secret session key. As a result, the non-hardened branch of line 13-17 is always taken while generating the message signature. Then the secret-dependent if -branch can leak out session key information. We present our evaluation results using page fault attack, B-SPM and T-SPM respectively, as follows:

Page-fault attacks.—During an offline analysis, we generated the sub-function call traces for both `_gcry_mpi_ec_dup_point` (Line 14 of Figure 4) and `_gcry_mpi_ec_add_points` (Line 16, a necessary condition for bit 1), from which we identified 4 code pages to be monitored, including `_gcry_mpi_ec_mul_point` on one page, `_gcry_mpi_ec_add_points` and `_gcry_mpi_ec_dup_point` on another page, their related functions on the third page and `_gcry_mpi_test_bit` on the last page, whose execution indicates the end of the processing on the current bit. During the attack, we intercepted the page fault handler in our kernel module and restricted accesses to these monitored pages by clearing their present bits. Once a page fault on a monitored page occurred we reset its present bit and recorded the current count of page faults. We found that for key bit 1 and 0, there are 89 and 48 subsequent page visits respectively. In total around 71,000 page faults were triggered to correctly recover all the session key bits.

B-SPM attacks.—We found that the aforementioned code page set is visited for both key bit 1 and 0, if we do not flush the TLB. Therefore, the spying thread needs to interrupt the target enclave thread and clean up the current TLB to get more detailed information about page visits to differentiate the key bit with different values. To reduce the frequency of the interrupts needed, instead of sending IPIs with fixed time interval, the spying thread runs simultaneously with the target thread and monitors a trigger page containing `ec_pow2` and `ec_mul2`. Whenever the trigger page is accessed, the spying thread interrupts the target thread to shoot down the TLB, and then identifies whether two other pages in the page set (000E9000 and 000F0000 in Table V) are visited between two interrupts. We observed a clear difference in the page traces for key bit 1 and 0 and can recover all key bits during the post-processing phase. In total around 33,000 interrupts were triggered to correctly recover all the session key bits.

T-SPM attacks.—To further reduce the AEX frequency, we monitor the 2 pages containing `_gcry_mpi_ec_mul_point` and `_gcry_mpi_ec_dup_point/_gcry_mpi_ec_add_points` respectively and utilize the time between the visits to both pages to find out the value of the current key bit. Specifically, once both of them are found to be accessed, our attack process starts the timer (using `rdtsc`) but waits for 2000 nanoseconds to ensure that the execution of the target process leaves both pages, before shooting down the TLB and resetting the *accessed* flags of both pages. The timer stops when

both pages are observed again. In this way, only about 2 interrupts are needed for collecting information for each key bit. The recorded timings turn out to be differentiating enough to determine whether `_gcry_mpi_ec_dup_point` or `_gcry_mpi_ec_add_points` has been executed, around 19,700 cpu cycles for the former and 27,900 cpu cycles for the latter. After all the call traces are gathered, we can figure out that the current key bit is 1 when `_gcry_mpi_ec_add_points` is observed right after `_gcry_mpi_ec_dup_point`, and 0 if only `_gcry_mpi_ec_dup_point` is seen. In total around 1,300 interrupts were triggered to correctly recover all the session key bits.

In summary, we found that these three attacks all are able to recover the full EdDSA session key reliably. Page fault attack triggers a page fault for every page observation and produces about 71,000 AEXs. The B-SPM attack can observe the page visit set between two consecutive inspections. However it still needs to aggressively send IPIs to clear TLB entries to gain timely observation of the pages visited, which produces about 33,000 AEXs. T-SPM attack only issues a TLB shutdown for every invocation of `_gcry_mpi_ec_dup_point` or `_gcry_mpi_ec_add_points` and differentiates between the two functions using timing information. As such, it generates a minimum number of AEXs. We noticed that a normal execution of the EdDSA program also incurs at least 1,500 page faults. The OS attacker could reduce the number of AEXs caused by normal page faults and therefore make the T-SPM attack unobservable.

V. Improving Spatial Granularity with Cache-DRAM ATTACKS

Page-fault side-channel attacks (and also the sneaky page monitoring attacks described in the previous section) only allow attackers to learn the enclave program's memory access patterns at a page granularity. Therefore, mechanisms that mix sensitive code and data into the same pages have been proposed to defeat such attacks [35]. Intel also recommends "aligning specific code and data blocks to exist entirely within a single page." [7]. However, the effectiveness of this defense method is heavily conditioned on the fact that page granularity is the best spatial granularity achievable by the adversary. However, our study suggests it is not the case.

In this section, we demonstrate three attack methods to show that a powerful adversary is able to improve spatial granularity significantly. Particularly, we will demonstrate a cross-enclave Prime+Probe cache attack, a cross-enclave DRAMA attack, and a cache-DRAM attack. Because SGX do not allow memory sharing between enclaves, the Flush+Reload cache attacks that can achieve cache-line granularity cannot be conducted against secure enclaves. However, we show that the cache-DRAM attack is capable of achieving the same level of spatial granularity against enclaves.

A. Cross-enclave Prime+Probe (Vector 7)

Our exploration starts with a validation of cross-enclave cache Prime+Probe attack. SGX is not designed to deal with cache side-channel attacks. Therefore, it is expected that known cache attacks also work against SGX enclaves. To confirm this, we ported GnuPG 1.4.13 to Graphene-SGX. The algorithm repeatedly decrypted a ciphertext which was encrypted with a 3,072-bit ElGamal public key, just as the prior work [27] did. GnuPG uses Wiener's table

to decide subgroup sizes matching field sizes and adds a 50% margin to the security parameters, consequently a private key of 403 bits is used. In the experiment an attack process monitored when the victim enclave was loaded and determined the physical address of Square-and-Multiply exponentiation. With knowledge of cache slicing and cache set mapping [21], the attacker constructed eviction sets mapped to the same cache sets as the target addresses. In our experiment, with the observation of only one ElGamal decryption, we could recover all 403 bits of the private key through a PRIME+PROBE cache attack with an error rate of 2.3%.

This experiment suggest that Prime+Probe cache attacks can be performed in a cross-enclave scenario, similar to the traditional settings. We note that Prime+Probe attacks achieves a spatial granularity of a cache set, which is 16KB on a processor with a 8196-set LLC (see Table I and Table VII).

B. Cross-enclave DRAMA (Vector 8)

The DRAMA attack exploits shared DRAM rows to extract sensitive information [32]. In such an attack, in order to learn whether the victim process has accessed a virtual address d , the adversary allocates two memory blocks that map to the same DRAM bank, with one sharing the same DRAM row with the physical memory of d , which we call p , and the other mapped to a different row on the same bank, which we call p' . The attack is conducted using the following steps:

- Access the memory block p' .
- Wait for some victim operations.
- Measure the access time of memory block p .

A faster memory access to memory block p suggests the victim process has probably touched memory address d during its operations. Of course, because the DRAM row is large (e.g., typically 8 KB), false detection is likely. Even so, DRAMA is shown to effectively detect the existence of keystroke activities [32].

Directly applying DRAMA to perform cross-enclave attacks faces several challenges, most of which are also faced by our design of cache-DRAM attacks. Therefore, we defer the discussion of these design challenges to Section V-C where we detail the cache-DRAM attacks. Here we enumerate some limitations of cross-enclave DRAMA attacks.

First, most of the victim's memory access will be cached (EPC is cacheable by default), and hence no information will be leaked through the use of DRAM rows. In fact, the original DRAMA paper only demonstrated the use of DRAMA to detect hardware events (e.g., keystrokes) that utilize non-cacheable memory regions [32]. While we could manually disable cache by setting the cache disable (CD) bit of CR0 for the core running the victim enclave³, this would slow down the enclave process for approximately 1000×.

³In Intel SGX programming reference [1] it is said that PRMRR_BASE register could be programmed with values UC(0×0) to set PRM range as uncacheable. We confirmed on our platform that PRMRR_BASE register cannot be changed after system boot.

Second, DRAMA attacks may falsely detect row hits that are unrelated to the victim enclave's visit to d , because the 8KB DRAM row can be shared by multiple data structure or code regions. This false detection, however, is very common in our experiments.

Finally, DRAMA cannot achieve fine-grained spatial accuracy. As an example, on our test system a memory page is distributed over 4 DRAM rows. In an extreme case the attacker could occupy an entire row except a single 1KB chunk for the victim enclave and achieve a spatial accuracy of 1KB (see Table VII), which is better than the PRIME+PROBE cache attack (16 KB), however still worse than a FLUSH+RELOAD cache attack (64B).

C. Cache-DRAM Attacks (Vector 7 & 8)

To improve cross-enclave DRAMA attacks, we propose a novel cache-DRAM attack. We show that by leveraging both vectors, the adversary can significantly improve the spatial granularity of memory side-channel attacks.

Techniques.—Particularly, the cache-DRAM attack is performed using two threads: one thread runs in non-enclave mode which PRIME+PROBES a cache set in the last-level cache in which the address d is mapped; the other thread conducts the cross-enclave DRAMA without disabling caching. As the PRIME+PROBE attack causes conflicts with d in the last-level cache, the victim enclave's accesses of d will reach the DRAM. The concept of cache-DRAM attack is shown in Figure 5. However, to implement cache-DRAM attacks against SGX enclaves, one needs to address the following challenges: *First, share the DRAM Bank and Row with d .* The EPC memory exclusively used by enclaves is already isolated from the rest of the physical memory in DRAMs. To understand this artifact, we explain the mechanism of the DRAM-level isolation using our own testbed (Table I) as an example. With the assumption of row bits being the most significant bits in a physical address [32], [38], any bit beyond bit 19 is a row bit that determines the corresponding DRAM row of the physical address. With a 128MB PRM (physical memory range 0×80000000 to $0 \times 87FFFFFF$), no non-PRM memory will occupy row number 0×1000 to $0 \times 10FF$, as shown in Table VI. As such, the PRM range (exclusively taken by enclaves) spans every DRAM bank and occupies specific sets of rows in each bank; these rows are not shared with non-PRM memory regions.

To overcome this barrier, we leverage the processor's support for running multiple enclave programs concurrently to carry out the DRAMA attacks from another enclave program controlled by the adversary. Since both programs operate inside enclaves, they share the EPC memory range. The adversary can manage to co-locate the memory page with the target enclave memory on the same banks and even the same rows, as illustrated in Figure 5. Specifically, we first identified the physical address of interest in the victim enclave. This can be achieved by reading the page tables directly. Then we allocated a large chunk of memory buffer in the spying enclave and determined their physical addresses. Using the reverse-engineering tool provided by the original DRAMA attack [32], we picked two memory addresses p and p' , as stated above. The attack is illustrated as in Figure 5. p and p' are accessed in turns without any delay. The access latency of memory block p is measured to determine whether the target address d in the victim enclave has just been visited.

Second, obtain fine-grained timers in enclaves. An unexpected challenge in executing this attack is the lack of a reliable clock. The SGXv1 processor family does not provide timing information within an enclave: the instructions such as `RDTSC` and `RDTSCP` are not valid for enclave programs. To measure time, a straightforward way is making system calls, which is heavyweight, slow and inaccurate, due to the variation in the time for processing `EEXIT` and calls. A much more lightweight solution we come up with utilizes the observation that an enclave process can access the memory outside without mode-switch. Therefore we can reserve a memory buffer for smuggling CPU cycle counts into the attack enclave. Specifically, a thread outside the enclave continuously dumps the cycle counts to the buffer and the attack thread inside continuously reads from the buffer. Although the race condition between them brings in noise occasionally due to our avoidance of mutex for supporting timely interactions between the threads, most of the time we successfully observed a timing difference between a row hit and a row conflict when probing the target enclave addresses. We use this method to measure the access latency of p .

Evaluation.—First we evaluate the accuracy of the timer we build for the attack. We designed a simple enclave process continuously visiting d with `clflush` instruction forcing the memory accesses to reach a DRAM row. An evaluator enclave utilized the timer to measure the access latency of p (the address on the same row as d), as well as the access latency of p' (the address on a different row), 1 million times each. Figure 6 shows the distributions of the access latency measured by the evaluator enclave during these accesses. As we see here the cases of DRAM row hit can be easily identified based on the timing difference observed through our timer (the left-most part of its distribution).

As an example, we ported Gap 4.8.6 to Graphene-SGX, targeting an input-dependent branch which is illustrated in Figure 7. Gap is a software package implementing various algebra algorithms. It uses a non-integer data type for values that cannot fit into 29 bits, otherwise the values are stored as immediate integers. In our experiment we had the victim enclave running the `SumInt` operation every $5 \mu s$. We set the range for a row hit detection as within 400-426 cpu cycles. To further reduce false positives brought by prefetching, we disabled hardware prefetches on the victim core by updating `MSR 0x1A4`. With the cache-DRAM attack targeting the instructions in line 8, our attack enclave could detect whether the branch in line 7 was taken with a probability of 14.6% and $<1\%$ false positive rate. Moreover, we only observed a 2% slowdown of enclave program in our experiment.

Discussion.—The cache-DRAM attack achieves a spatial accuracy of 64 byte which is as accurate as the `Flush+Reload` cache attacks. In the meanwhile it ensures that only the targeted cache set is primed which further reduces the false positives caused by accesses of shared DRAM rows. The attack can be more powerful for a dedicated attacker by reserving a DRAM bank exclusively for the victim and spying enclaves.

VI. Mitigation and Discussion

A. Analysis of Attack Surfaces

Table VII summarizes the characteristics of the memory side-channel attacks discovered over different vectors. The data here were collected from the system configuration in Table I and a PRM size of 128MB. The value under the *Accuracy* column shows the spatial accuracy of the attack vectors. For example, the iCache PRIME+PROBE channel has an accuracy of 2MB (i.e., 128MB/64): that is, detecting one cache miss in one of the iCache sets could probably mean any of 2MB of the physical memory being accessed. The larger the number is, the coarser-grained the vector will be. The attack with the finest granularity is the cache-DRAM attack, which is 64 bytes, equivalent to the FLUSH+RELOAD cache attacks. However, note that due to lack of shared memory pages—as EPC pages only belong to one enclave at a time—FLUSH+RELOAD cache attacks are not feasible on SGX enclaves. It is also worth noting that the calculation of the accuracy does not consider knowledge of the physical memory exclusively used by the target enclave. This information can help improve the granularity even further. PRIME+PROBE cache attacks on iCache, dCache and L2 cache induce high volume of AEXs. This does not take HyperThreading into consideration. If so, both AEX numbers and slowdowns will become *modest*. Most of the attack vectors that need to frequently preempt the enclave execution will induce *high* overheads. The cross-enclave DRAMA needs to disable cache to conduct effective attacks, therefore inducing *high* slowdown. What is not shown in the table is *temporal observabilities*. Except for page-fault attacks, all other attacks have temporal observabilities, as they allow observing finer-grained information than allowed by their basic information unit, which are leaked through timing signals.

Other attack vectors not listed.—FLUSH+RELOAD cache attacks against cached PTE entries are one attack vector that we have not listed in Table VII. As a PTE entry shares cache line with 7 more PTE entries, the spatial accuracy is $4\text{KB} \times 8 = 32\text{KB}$. The attack can achieve the spatial accuracy of 4KB if PTE entries are intentionally organized. Combining SPM and DRAMA attacks will also introduce a new attack vector. We did not show these attacks due to the similarity to the ones we demonstrated.

B. Effectiveness of Existing Defenses

Deterministic multiplexing.—Shinde *et al.* [35] proposes a compiler-based approach to opportunistically place all secret-dependent control flows and data flows into the same pages, so that page-level attacks will not leak sensitive information. However, this approach does not consider cache side channels or DRAM side channels, leaving the defense vulnerable to cache attacks and DRAMA.

Hiding page faults with transactional memory.—T-SGX [34] prevents information leakage about page faults inside enclaves by encapsulating the program’s execution inside hardware-supported memory transactions. Page faults will cause transaction aborts, which will be handled by abort handler inside the enclave first. The transaction abort handler will notice the abnormal page fault and decide whether to forward the control flow to the untrusted OS kernel. As such, the page fault handler can only see that the page fault happens

on the page where the abort handler is located (via register CR2). The true faulting address is hidden.

However, T-SGX cannot prevent the *accessed* flags enabled memory side-channel attacks. According to Intel Software Developer's manual [3], transaction abort is not strictly enforced when the *accessed* flags and *dirty* flags of the referenced page table entry is updated. This means there is no security guarantee that memory access inside transactional region is not leaked through updates of the page table entries.

Secure processor design.—Sanctum [15] is a new hardware design that aims to protect against both last-level cache attacks and page-table based attacks. As Sanctum enclave has its own page tables, page access patterns become invisible to the malicious OS. Therefore, the page-faults attacks and SPM attacks will fail. However, Sanctum does not prevent cross-enclave DRAMA attack. As a matter of fact, Sanctum still relies on the OS to assign DRAM regions to enclaves, create page table entries and copy code and data into the enclave during enclave initialization. Since OS knows the exact memory layout of the enclave, the attacker can therefore run an attack process in a different DRAM region that shares a same DRAM row as the target enclave address.

Timed execution.—Chen *et al.* [14] proposes a compiler-based approach, called DÉJÀ VU, to measure the execution time of an enclave program at the granularity of basic blocks in a control-flow graph. Execution time larger than a threshold indicates that the enclave code has been interrupted and AEX has occurred. The intuition behind it is that execution time measured at the basic block level will not suffer from the variations caused by different inputs. Due to the lack of timing measurements in SGX v1 enclaves, DÉJÀ VU constructs a software clock inside the enclave which is encapsulated inside Intel Transactional Synchronization Extensions (TSX). Therefore, the clock itself will not be interrupted without being detected. It was shown that DÉJÀ VU can detect AEX with high fidelity. Therefore, any of the side-channel attack vectors that induce high volume of AEX will be detected by DÉJÀ VU. However, those not involving AEX in the attacks, such as SPM attacks will bypass DÉJÀ VU completely.

Enclave Address Space Layout Randomization.—SGX-Shield [33] implemented fine-grained ASLR when an enclave program is loaded into the SGX memory. However the malicious OS could still learn the memory layout after observing memory access patterns in a long run as SGX-Shield does not support live re-randomization.

C. Lessons Learned

Our systematic analysis of SGX memory side channels brings to light new attack surfaces and new capabilities the adversary has. Here are a few thoughts about how to mitigate such risks on the SGX platform, and more generically, for the emerging TEE.

SGX application development.—Our research shows that the adversary can achieve fine-grained monitoring of an enclave process, through not only pages and cache channels, but also inter-page timing, cross-enclave DRAM and HyperThreading. It is important for the SGX developer to realize the impacts of these new attack surfaces, which is critical for

building enclave applications to avoid leaks through the new channels. For example, she can no longer hide her secret by avoiding page-level access patterns, since intra- or inter-page timings can also disclose her sensitive information.

Software-level protection.—Defense against SGX side-channel leaks can no longer rely on the assumptions we have today. Particularly, such attacks do not necessarily cause an anomalously high AEX rate. Blending sensitive information into the same memory pages is not effective against attacks with finer spatial granularity. Also, the adversary may also use a combination of multiple channels to conduct more powerful attacks.

Hardware enhancement.—Most memory side channels we know so far can be mitigated through hardware changes, e.g., partitions of caches/DRAM and keeping enclave page tables inside EPC, etc. In some cases, such changes could be the best option. Further research is expected to better understand the issue and the impacts of the related side channels, making the case to Intel and other TEE manufacturers for providing hardware-level supports.

Big picture.—Over years, we observe that many side-channel studies follow a similar pattern: a clever attack is discovered and then researchers immediately embark on the defense against the attack. However, in retrospection, most defense proposals fail to consider the bigger picture behind the demonstrated attacks, thus they are unable to offer effective protection against the adversary capable of quickly adjusting strategies, sometimes not even meaningfully raising the bar to the variations of the attacks. The ongoing research on SGX apparently succumbs to the same pitfalls. We hope that our study can serve as a new start point for rethinking the ongoing effort on SGX security, inspiring the follow-up efforts to better understand the fundamental limitations of this new TEE and the ways we can use it effectively and securely.

VII. Related Work

Side-Channel Attacks on SGX.

It has been shown in previous studies that page-level memory access patterns can leak secrets of enclave programs under a variety of scenarios [39], [35]. This type of leakage is enabled by enforcing page faults during enclave's execution, by marking selected memory pages to be non-present or non-executable. As such, data accesses or code execution in these pages will thus be trapped into the OS kernel, and so the malicious OS will learn which page is accessed by the enclave program. Page-fault side-channel attack is one attack vector of the memory side-channel attack surface we explore in this paper.

A very recent study explores branch prediction units as side channels to infer sensitive control flows inside SGX enclaves [25]. The memory side-channel attack surface does not include attack vectors through branch prediction. Both are important to the understanding of side-channel security of Intel SGX.

Cache Side Channels.

Cache side-channel attacks under the threat model we consider in this proposal (i.e., access driven attacks [17]) have been demonstrated on x86 architectures, including data caches (and

also per-core L2 unified caches) [31], [30], [28], [36], [17], [18], instruction caches [8], [9], [43], and inclusive LLCs [41], [40], [12], [44], [22], [27], [20], [16], [29], [19], [23], [26], [42]. The studies on these cache side channels are still valid on SGX enclaves. We briefly confirmed the effectiveness of cache side-channel attacks in our paper, while the focus of this work is a broader attacker surface than cache.

VIII. Conclusion

We report the first systematic analysis of SGX memory side channels in the paper. Our study identified 8 attack vectors in memory management, ranging from TLB to DRAM. Further we demonstrate a set of novel attacks that exploit these channels, by leveraging *accessed* flags, timing, HyperThreading and DRAM modules. Compared with the page-fault attack, the new attacks are found to be stealthier and much more lightweight, with effectiveness comparable with the known attack in some cases. Most importantly, our study broadens the scope of side-channel studies on SGX, reveals the gap between proposed defense and the design weaknesses of the system, and can provoke the further discussion on how to use the new TEE techniques effectively and securely.

References

- [1]. Intel software guard extensions programming reference. <https://software.intel.com/sites/default/files/managed/48/88/329298-002.pdf>, 2014. Order Number: 329298-002, 10 2014.
- [2]. Intel software guard extensions (intel sgx). <https://software.intel.com/sites/default/files/332680-001.pdf>, 2015 6 2015.
- [3]. Intel 64 and IA-32 architectures software developer’s manual, combined volumes:1,2A,2B,2C,3A, 3B,3C and 3D. <https://software.intel.com/sites/default/files/managed/3/9/c5/325462-sdm-vol-1-2abcd-3abcd.pdf>, 2016. Order Number: 325462-061US, 12 2016.
- [4]. Intel 64 and IA-32 architectures software developer’s manual, combined volumes:1,2A,2B,2C,3A, 3B,3C and 3D, 2016. Order Number: 325462-058US 4 2016.
- [5]. Graphene / graphene-sgx library os - a library os for linux multi-process applications, with intel sgx support. <https://github.com/oscarlab/graphene/>, 2017 Accessed May 16, 2017.
- [6]. Intel sgx and side-channels. <https://software.intel.com/en-us/articles/intel-sgx-and-side-channels>, 2017. Added 3 26, 2017.
- [7]. Intel software guard extensions enclave writer’s guide. <https://software.intel.com/sites/default/files/managed/ae/48/Software-Guard-Extensions-Enclave-Writers-Guide.pdf>, 2017 Revision 1.02, Accessed May, 2017.
- [8]. Aciicmez Onur. Yet another microarchitectural attack: exploiting I-Cache. In ACM workshop on Computer security architecture, 2007.
- [9]. Aciicmez Onur, Brumley Billy Bob, and Grabher Philipp. New results on instruction cache attacks. In 12th international conference on Cryptographic hardware and embedded systems, 2010.
- [10]. Anati Ittai, Gueron Shay, Johnson Simon, and Scarlata Vincent. Innovative technology for cpu based attestation and sealing. In Proceedings of the 2nd international workshop on hardware and architectural support for security and privacy, volume 13, 2013.
- [11]. Akkary Haitham Glew Andy, Hinton Glenn. Method and apparatus for performing page table walks in a microprocessor capable of processing speculative instructions. US Patent 5680565 A, 1997.
- [12]. Benger Naomi, Pol Joop van de, Smart Nigel P., and Yarom Yuval. “Ooh Aah... Just a Little Bit”: A small amount of side channel can go a long way. In 16th International Workshop on Cryptographic Hardware and Embedded Systems, 2014.
- [13]. Daniel J Bernstein Niels Duif, Lange Tanja, Schwabe Peter, and Yang Bo-Yin. High-speed high-security signatures. Journal of Cryptographic Engineering, pages 1–13, 2012.

- [14]. Chen Sanchuan, Zhang Xiaokuan, Reiter Michael, and Zhang Yinqian. Detecting privileged side-channel attacks in shielded execution with DÉJÀ VU. In 12th ACM Symposium on Information, Computer and Communications Security, 2017.
- [15]. Costan Victor, Lebedev Ilia, and Devadas Srinivas. Sanctum: Minimal hardware extensions for strong software isolation. In 25th USENIX Security Symposium USENIX Association, 2016.
- [16]. Gruss Daniel, Spreitzer Raphael, and Mangard Stefan. Cache template attacks: Automating attacks on inclusive last-level caches. In 24th USENIX Security Symposium, 2015.
- [17]. Gullasch D, Bangerter E, and Krenn S Cache games – bringing access-based cache attacks on AES to practice. In 32nd IEEE Symposium on Security and Privacy, 2011.
- [18]. Hund Ralf, Willems Carsten, and Holz Thorsten. Practical timing side channel attacks against kernel space ASLR. In 34th IEEE Symposium on Security and Privacy, 2013.
- [19]. Inci Mehmet Sinan, Gulmezoglu Berk, Irazoqui Gorka, Eisenbarth Thomas, and Sunar Berk. Seriously, get off my cloud! cross-VM RSA key recovery in a public cloud. Cryptology ePrint Archive, 2015.
- [20]. Irazoqui Gorka, Eisenbarth Thomas, and Sunar Berk. S\$A: A shared cache attack that works across cores and defies VM sandboxing—and its application to AES. In IEEE Symposium on Security and Privacy, 2015.
- [21]. Irazoqui Gorka, Eisenbarth Thomas, and Sunar Berk. Systematic reverse engineering of cache slice selection in intel processors. In Digital System Design (DSD), 2015 Euromicro Conference on, pages 629–636. IEEE, 2015.
- [22]. Irazoqui Gorka, Inci Mehmet Sinan, Eisenbarth Thomas, , and Sunar Berk. Wait a minute! a fast, cross-vm attack on AES. In 17th International Symposium Research in Attacks, Intrusions and Defenses, 2014.
- [23]. Kayaalp Mehmet, Nael Abu-Ghazaleh Dmitry Ponomarev, and Jaleel Aamer. A high-resolution side-channel attack on last-level cache. In 53rd Annual Design Automation Conference, 2016.
- [24]. Lamson Butler W.. A note on the confinement problem. *Commun. ACM*, 16(10), 10 1973.
- [25]. Lee Sangho, Shih Ming-Wei, Gera Prasun, Kim Taesoo, Kim Hyesoon, and Peinado Marcus. Inferring fine-grained control flow inside SGX enclaves with branch shadowing. *CoRR*, abs/1611.06952, 2016.
- [26]. Lipp Moritz, Gruss Daniel, Spreitzer Raphael, Maurice Clémentine, and Mangard Stefan. Armageddon: Cache attacks on mobile devices. In USENIX Security Symposium, 2016.
- [27]. Liu Fangfei, Yarom Yuval, Ge Qian, Heiser Gernot, and Lee Ruby B. Last-level cache side-channel attacks are practical. In IEEE Symposium on Security and Privacy, 2015.
- [28]. Neve Michael and Seifert Jean-Pierre. Advances on access-driven cache attacks on AES. In 13th international conference on selected areas in cryptography, 2007.
- [29]. Oren Yossef, Kemerlis Vasileios P., Sethumadhavan Simha, and Keromytis Angelos D. The spy in the sandbox: Practical cache attacks in javascript and their implications. In 22nd ACM SIGSAC Conference on Computer and Communications Security, 2015.
- [30]. Osvik Dag Arne, Shamir Adi, and Tromer Eran. Cache attacks and countermeasures: the case of AES. In 6th Cryptographers’ track at the RSA conference on Topics in Cryptology, 2006.
- [31]. Percival Colin. Cache missing for fun and profit. In BSDCon 2005, 2005.
- [32]. Pessl Peter, Gruss Daniel, Maurice Clementine, Schwarz Michael, and Mangard Stefan. Drama: Exploiting dram addressing for cross-cpu attacks. In Proceedings of the 25th USENIX Security Symposium, 2016.
- [33]. Seo Jaebaek, Lee Byoungyoung, Kim Sungmin, Shih Ming-Wei, Shin Insik, Han Dongsu, and Kim Taesoo. SGX-Shield: Enabling Address Space Layout Randomization for SGX Programs (to appear). In Proceedings of the 2017 Annual Network and Distributed System Security Symposium (NDSS), San Diego, CA, 2 2017.
- [34]. Shih Ming-Wei, Lee Sangho, Kim Taesoo, and Peinado Marcus. T-SGX: Eradicating Controlled-Channel Attacks Against Enclave Programs (to appear). In Proceedings of the 2017 Annual Network and Distributed System Security Symposium (NDSS), San Diego, CA, 2 2017.
- [35]. Shinde Shweta, Zheng Leong Chua Viswesh Narayanan, and Saxena Prateek. Preventing page faults from telling your secrets. In 11th ACM Symposium on Information, Computer and Communications Security, 2016.

- [36]. Tromer Eran, Osvik Dag Arne, and Shamir Adi. Efficient cache attacks on AES, and countermeasures. *Journal of Cryptology*, 23(2):37–71, 1 2010.
- [37]. Tsai Chia-Che, Kumar Saurabh Arora Nehal Bandi, Jain Bhushan, Jannen William, John Jitin, Harry A Kalodner Vrushali Kulkarni, Oliveira Daniela, and Porter Donald E. Cooperation and security isolation of library oses for multi-process applications. In *Proceedings of the Ninth European Conference on Computer Systems*, page 9 ACM, 2014.
- [38]. Xiao Yuan, Zhang Xiaokuan, Zhang Yinqian, and Teodorescu Radu. One bit flips, one cloud flops: Cross-vm row hammer attacks and privilege escalation. In *USENIX Security Symposium*, 2016.
- [39]. Xu Yuanzhong, Cui Weidong, and Peinado Marcus. Controlled-channel attacks: Deterministic side channels for untrusted operating systems. In *36th IEEE Symposium on Security and Privacy*, 2015.
- [40]. Yarom Yuval and Bengier Naomi. Recovering OpenSSL ECDSA nonces using the FLUSH +RELOAD cache side-channel attack. In *Cryptology ePrint Archive*, 2014.
- [41]. Yarom Yuval and Falkner Katrina. Flush+reload: A high resolution, low noise, L3 cache side-channel attack. In *USENIX Security Symposium*, 2014.
- [42]. Zhang Xiaokuan, Xiao Yuan, and Zhang Yinqian. Return-oriented flush-reload side channels on arm and their implications for android devices. In *ACM Conference on Computer and Communications Security*, 2016.
- [43]. Zhang Yinqian, Juels Ari, Reiter Michael K., and Ristenpart Thomas. Cross-VM side channels and their use to extract private keys. In *ACM Conference on Computer and Communications Security*, 2012.
- [44]. Zhang Yinqian, Juels Ari, Reiter Michael K., and Ristenpart Thomas. Cross-tenant side-channel attacks in PaaS clouds. In *ACM Conference on Computer and Communications Security*, 2014.

	63	62		52	51				12	11		9	8	7	6	5	4	3	2	1	0
X													G	P	D	A	C	W	U	R	
D													S	S	D	T	D	T	S	W	P

Fig. 1.
Page table entries.

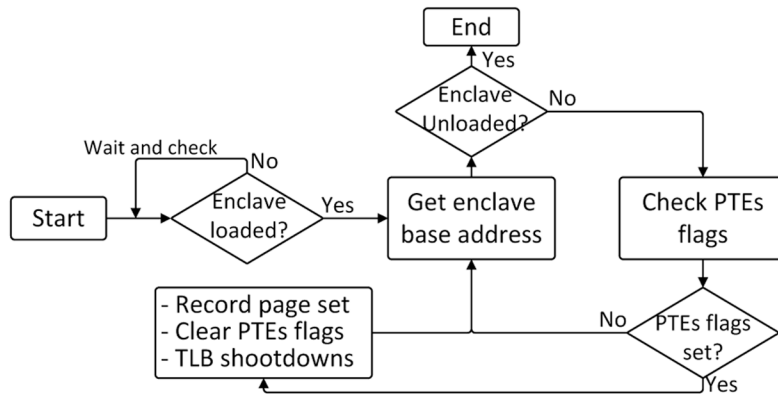


Fig. 2.
Basic SPM attack.

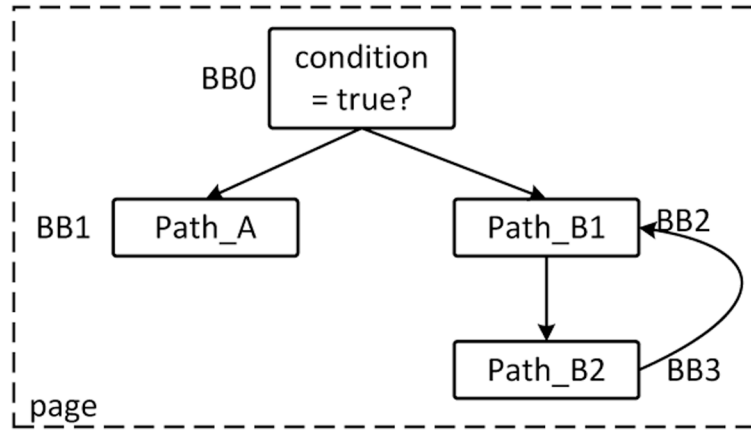


Fig. 3. An example of secret-dependent branch leaking timing information.

```
1 void
2 _gcry_mpi_ec_mul_point (mpi_point_t result,
3                        gcry_mpi_t scalar, mpi_point_t
4                        point,
5                        mpi_ec_t ctx) {
6   if (ctx->model == MPI_EC_EDWARDS
7       || (ctx->model == MPI_EC_WEIERSTRASS
8           && mpi_is_secure (scalar))) {
9     if (mpi_is_secure (scalar)) {
10      /* If SCALAR is in secure memory we assume that
11         it is the secret key we use constant time
12         operation. */
13      ...
14     }
15     else {
16       for (j=nbits-1; j >= 0; j--) {
17         _gcry_mpi_ec_dup_point (result, result, ctx);
18         if (mpi_test_bit (scalar, j))
19           _gcry_mpi_ec_add_points (result, result,
20                                   point, ctx);
21       }
22     }
23   }
24   return;
25 }
```

Fig. 4.
Scalar point multiplication for ECC.

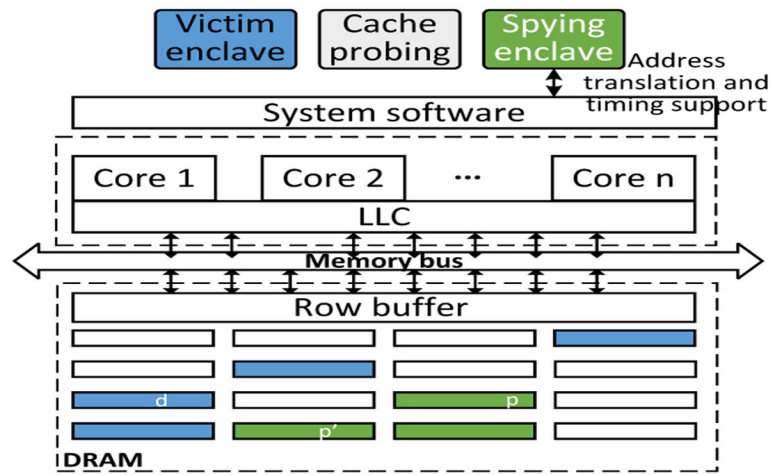


Fig. 5. Illustration of cache-DRAM attack.

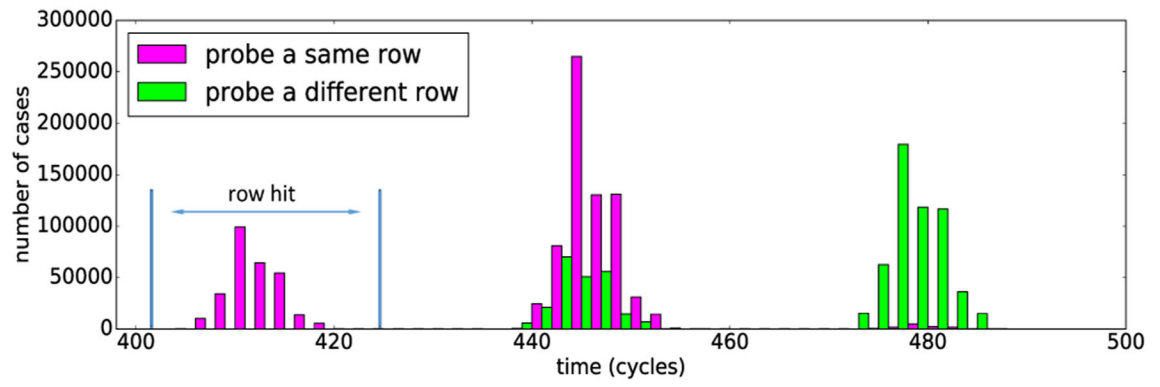


Fig. 6.
Distribution of access latency for probing the same row and a different row.

```
1 /*An input dependent branch from gap library*/
2 Obj SumInt(Obj opL, Obj opR) {
3   // initialize temp variables
4   // ...
5
6   // adding two small integers
7   if( ARE_INTOBJJS( opL, opR) ) {
8     if(SUM_INTOBJJS(sum, opL, opR))
9       return sum;
10    cs = INT_INTOBJ(opL)+INT_INTOBJ(opR);
11    // ...
12  }
13  // adding one large integer and small integer
14  else if( IS_INTOBJ(opL) || IS_INTOBJ(opR) ) {
15    // ...
16  }
17  // add two large integers
18  else {
19    // ...
20  }
21 }
```

Fig. 7.
An input-dependent branch in Gap 4.8.6.

TABLE I

CONFIGURATION OF THE TESTBED.

	Size	Sets \times Ways
iTLB	64	8×8
dTLB	64	16×4
L2 TLB	1536	256×6
iCache	32KB	64×8
dCache	32KB	64×8
L2 Cache	256KB	1024×4
L3 Cache	8MB	8192×16
	Size	Channel \times DIMMs \times Ranks \times Banks \times Rows
DRAM	8GB \times 2	$2 \times 1 \times 2 \times 16 \times 2^{15}$

Author Manuscript

Author Manuscript

Author Manuscript

Author Manuscript

TABLE II

WORDS DISTRIBUTION IN THE EN_US HUNSPELL DICTIONARY.

group size	Page-fault based		Accessed-flag based	
	words	%	words	%
1	51599	83.05	45649	73.47
2	7586	12.21	8524	13.72
3	2073	3.34	3027	4.87
4	568	0.91	1596	2.57
5	200	0.32	980	1.58
6	60	0.10	810	1.30
7	35	0.06	476	0.77
8	8	0.01	448	0.72
9	0	0	306	0.49
10	0	0	140	0.23
>10	0	0	173	0.28

Author Manuscript

Author Manuscript

Author Manuscript

Author Manuscript

TABLE III

FEATURES USED IN FREETYPE EXPERIMENT.

trigger page	0×0005B000
	0005B000, 0005B000
	0005B000, 00065000
α - β pairs	0005B000, 0005E000
	00065000, 00022000
	0005E000, 00018000

Author Manuscript

Author Manuscript

Author Manuscript

Author Manuscript

TABLE IV

T-SPM ATTACK ON FREETYPE 2.5.3: FOR EXAMPLE, WE ACHIEVED A PRECISION OF 69.90% OVER A COVERAGE OF 100% CHARACTERS.

coverage	100%	88.17%	75.62%	69.14%	57.35%
precision	69.90%	75.25%	80.66%	84.45%	89.94%

Author Manuscript

Author Manuscript

Author Manuscript

Author Manuscript

TABLE V

ATTACK SUMMARY ON EdDSA (LIBGCRYPT 1.7.5). A NORMAL EXECUTION OF EdDSA SIGNATURE WITHOUT ATTACK ALSO INCURS OVER 1500 AEXS.

	Monitored pages	Number of AEXs
Page fault attack	000E7000, 000E8000 000F0000, 000F1000	71,000
B-SPM attack	000EF000 (trigger page) 000E9000, 000F0000	33,000
T-SPM attack	000F0000 (trigger page) 000F1000 (trigger page)	1,300

Author Manuscript

Author Manuscript

Author Manuscript

Author Manuscript

TABLE VI

ROW RANGES FOR DIFFERENT PRM SIZE.

PRM size	PRM range	DRAM row range
32MB	0x88000000~0x89FFFFFF	0x1100~0x113F
64MB	0x88000000~0x8BFFFFFF	0x1100~0x117F
128MB	0x80000000~0x87FFFFFF	0x1000~0x10FF

Author Manuscript

Author Manuscript

Author Manuscript

Author Manuscript

TABLE VII

ANALYSIS OF SIDE-CHANNEL ATTACK SURFACES.

Vectors	Accuracy	AEX	Slowdown
i/dCache PRIME+PROBE	2MB	high	high
L2 Cache PRIME+PROBE	128KB	high	high
L3 Cache PRIME+PROBE	16KB	none	modest
page faults	4KB	high	high
B/T-SPM	4KB	modest	modest
HT-SPM	4KB	none	modest
cross-enclave DRAMA	1KB	none	high
cache-DRAM	64B	none	minimal

Author Manuscript

Author Manuscript

Author Manuscript

Author Manuscript